Boualem Boashash, Ghasem Azemi, and John M. O'Toole

Time-Frequency Processing of Nonstationary Signals

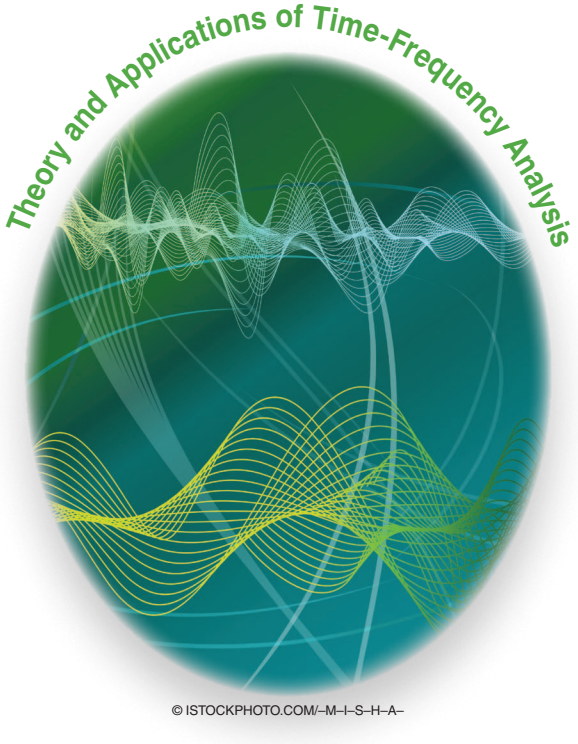

Advanced TFD design to aid diagnosis with highlights from medical applications

This article presents a methodical approach for improving quadratic time-frequency distribution (QTFD) methods by designing adapted time-frequency (T-F) kernels for diagnosis applications with illustrations on three selected medical applications using the electroencephalogram (EEG), heart rate variability (HRV), and pathological speech signals. Manual and visual inspection of such nonstationary multicomponent signals is laborious especially for long recordings, requiring skilled interpreters with possible subjective judgments and errors. Automated assessment is therefore preferred for objective diagnosis by using T-F distributions (TFDs) to extract more information. This requires designing advanced high-resolution TFDs for automating classification and interpretation. As QTFD methods are general and their coverage is very broad, this article concentrates on methodologies using only a few selected medical problems studied by the authors.

Digital Object Identifier 10.1109/MSP.2013.2265914
Date of publication: 15 October 2013

1053-5888/13/$31.00©2013IEEE

INTRODUCTION AND BACKGROUND

BACKGROUND

Analysis, detection, and classification are required in many applications where signals are nonstationary and/or multicomponent [1]. High-resolution T-F analysis and instantaneous frequency (IF)-based techniques were shown to be suitable for such signals [1]–[5]. These methods are often quadratic and can be defined as estimates of the power spectral density (PSD) in the nonstationary case [1, pp. 36–38]. They are referred to as *TFDs* and can be considered as smoothed versions of the Wigner–Ville distribution (WVD). For given analytic signals $z_{x_1}(t)$ and $z_{x_2}(t)$ associated with real signals $x_1(t)$ and $x_2(t)$; i.e.,

$$z_{x_i}(t) = x_i(t) + j\mathcal{H}\{\mathrm{x_i}(t)\};\ i = 1, 2 \tag{1}$$

with $\mathcal{H}\{\,\}$ being the Hilbert transform, the cross-WVD (XWVD) is defined as [1, p. 64]

$$W_{z_{x_1}z_{x_2}}(t,f) = \int_{-\infty}^{\infty} z_{x_1}\left(t+\frac{\tau}{2}\right) z_{x_2}^{*}\left(t-\frac{\tau}{2}\right) \mathrm{e}^{-\mathrm{j}2\pi f\tau}\,\mathrm{d}\tau. \tag{2}$$

For $z_{x_1}(t) = z_{x_2}(t) = z(t)$, (2) represents the WVD of $z(t)$, $W_z(t,f)$. With $\mathcal{F}\{\,\}$ being the Fourier transform (FT), the general formula for a QTFD with T-F kernel $\gamma(t,f)$ and Doppler-lag kernel $g(\nu,\tau) = \mathcal{F}_{t\to\nu}\{\mathcal{F}^{-1}_{f\to\tau}\{\gamma(t,f)\}\}$ of the analytic signal $z(t)$ is given by [1]

$$\begin{aligned}\rho_z(t,f) &= W_z(t,f) \mathop{**}_{t\ f} \gamma(t,f)\\ &= \mathop{\mathcal{F}^{-1}}_{\nu\to t}\left\{\mathop{\mathcal{F}}_{\tau\to f}\{g(\nu,\tau)A_z(\nu,\tau)\}\right\},\end{aligned} \tag{3}$$

where $A_z(\nu,\tau)$ is the symmetric ambiguity function (SAF) of $z(t)$, expressed as

$$A_z(\nu,\tau) = \int_{-\infty}^{\infty} z\left(t+\frac{\tau}{2}\right) z^{*}\left(t-\frac{\tau}{2}\right) \mathrm{e}^{-\mathrm{j}2\pi\nu t}\,\mathrm{d}t. \tag{4}$$

For TFDs with separable kernels, $g(\nu,\tau)$ can be written as $g(\nu,\tau) = G_1(\nu)g_2(\tau)$.

This article formulates enhanced QTFD methods by designing adapted T-F kernels $\gamma(t,f)$ or equivalently their two-dimensional (2-D)-FT $g(\nu,\tau)$ for selected medical applications. Although this article focuses on QTFDs, other T-F techniques presented in this special issue of *IEEE Signal Processing Magazine,* such as reassignment and synchrosqueezing, can also be used to enhance T-F representation of multicomponent signals.

KEY T-F NOVELTIES AND DIAGNOSTIC APPLICATIONS

In the section "Designing High-Resolution Quadratic TFDs," we introduce an advanced formulation of high-resolution QTFDs [1, Sec. 6.1], [6] for analysis of multicomponent signals and methods for fast computation, with illustration by selected medical issues [7]. Examples of such TFDs in Figure 1 show multicomponents, nonstationarity, and harmonics in a newborn's EEG and HRV signals.

The problem of detecting a specific signal abnormality such as a seizure in a newborn's EEG is considered in the section "Time-Frequency Detection of Abnormalities in Nonstationary Signals." Using specific T-F matched filters (TFMFs) [8], [9], experimental results on multichannel newborn EEGs show significant improvements over time-domain matched filters using the area under the curve (AUC) values as a detection metric. In the section "T-F-Based Features for Classifying Multicomponent Nonstationary Signals," features

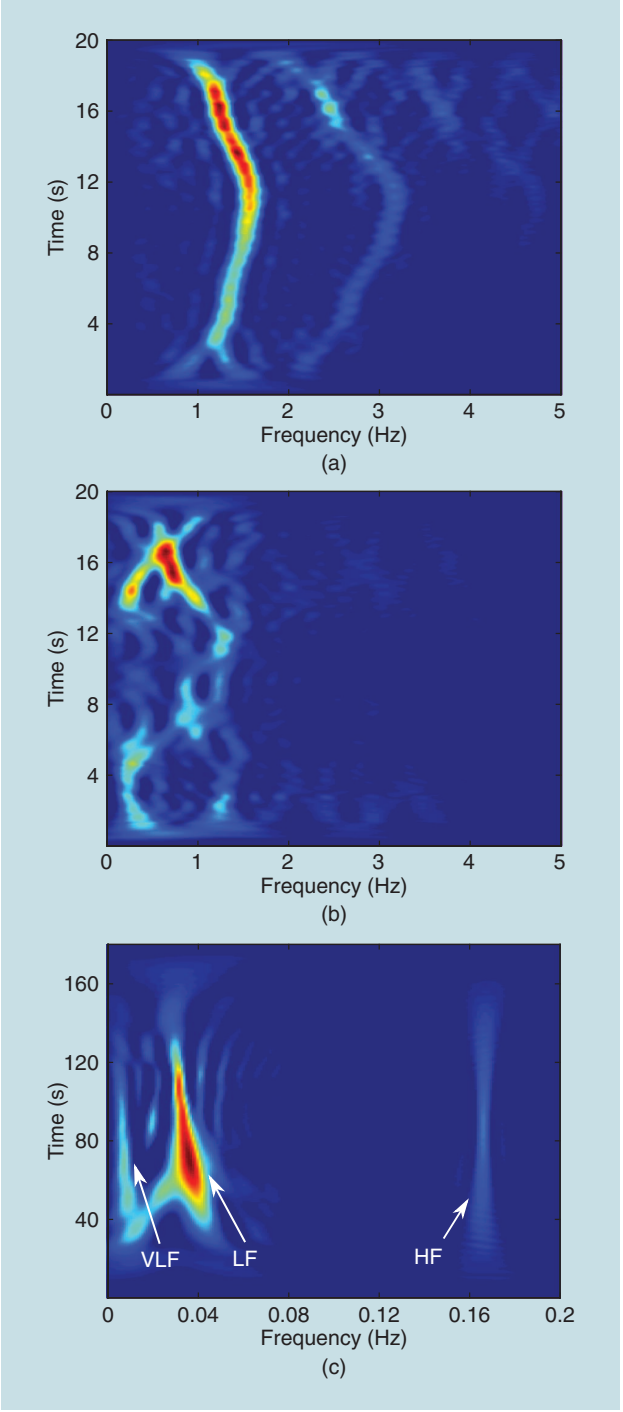

[FIG1] TFDs of an epoch of (a) a newborn's EEG with a seizure, (b) a newborn's EEG background, and (c) HRV signals.

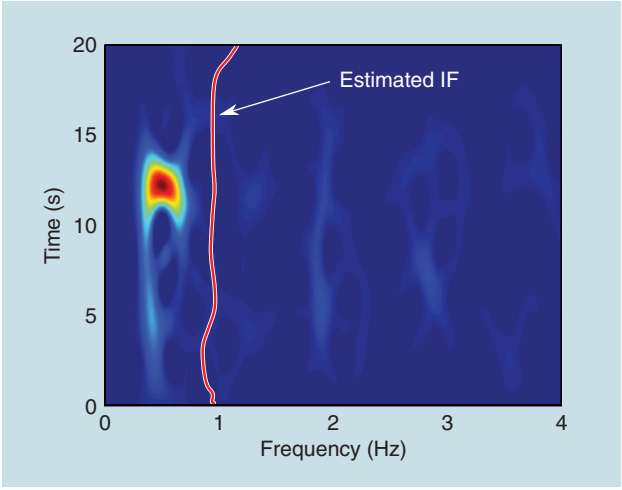

[FIG2] The TFD of an EEG epoch with periodic lateralized epileptiforms (PLEDs) with known IF law around 1 Hz. Estimated IF overlays the TFD. Note that the estimated IF does not follow the peaks of the TFD.

for classifying nonstationary signals are presented using the extra information in the T-F domain that identify the signal nonstationary characteristics [8]. T-F-based methods for diagnosis of other medical abnormalities using EEG, HRV, and pathological speech (which are all both nonstationary and multicomponent [1], [4], [10]–[12]) are illustrated in the section "Examples of T-F Applications for Automating Medical Abnormality Diagnosis."

SIGNALS CONSIDERED

Several kind of physiological signals are considered in this article (see Figures 1–3). Scalp EEG is the manifestation of combined brain sources and used to monitor the central nervous system for diagnosis and prognosis of brain damage. HRV is the beat-to-beat oscillations in the heart rate signal [13]; it includes three frequency components; i.e., high

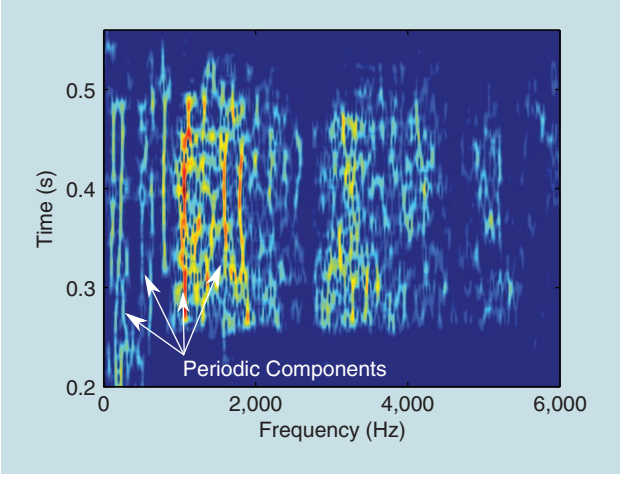

[FIG3] The TFD of the enhanced oesophageal speech signal, of the word "mama." Periodic components (LFM-type signals) are retained in the voiced segments to improve HNR.

frequency (HF), low frequency (LF), and very low frequency (VLF) [13] [Figure 1(c)]. Pathological oesophageal speech is an abnormal mode of speech for people without a larynx, requiring enhancement.

METHODS CONSIDERED

Several types of T-F methods are used in this article. Detection of a newborn seizure using EEG signals, T-F matched filtering, and T-F feature recognition can be improved by using findings that newborn EEG seizures may be modeled as piecewise linear frequency modulated (LFM) signals with harmonics [9]. Another method uses TFD and IF-based measures for assessing phase asynchrony in multichannel EEG signals [14]–[16]. An EEG methodology uses the IF as a feature to classify different epileptiform discharges in (adult) EEG, using a T-F peak-tracking method for IF estimation, and removing spectral modulation by homomorphic filtering in the T-F domain. High-resolution QTFDs are used to enhance pathological oesophageal speech and improve the quality and intelligibility of these signals.

These theoretical developments and techniques are presented next in more detail to highlight the importance of continuing to develop, adapt, and apply new high-resolution T-F methods for diagnostic applications such as detecting medical abnormalities to help improve health outcomes.

DESIGNING HIGH-RESOLUTION QUADRATIC TFDs

MULTICOMPONENT NONSTATIONARY AM–FM SIGNAL MODEL

Unlike monocomponent signals, nonstationary multicomponent signals are characterized in the T-F domain by several ridges corresponding to several IF laws, as observed in Figure 1. Such signals can therefore be modeled as a sum of monocomponent signals [1]

$$z_K(t) = \sum_{k=1}^{K} z_k(t) = \sum_{k=1}^{K} a_k(t) e^{j\phi_k(t)}, \tag{5}$$

where K is the number of signal components and $z_k(t)$ represents the analytic associate of the signal kth component [see (1)] with the instantaneous phase (IP) $\phi_k(t)$ and instantaneous amplitude (IA) $a_k(t)$. The IF of the monocomponent signal $z_k(t)$ is defined as $f_k(t) = \phi_k'(t)/2\pi$ and can be estimated using the peak of the TFD of $z_k(t)$ as $\hat{f}_k(t) = \arg\{\max_f \rho_{z_k}(t, f)\}$, where $\rho_{z_k}(t, f)$ is the TFD of the signal component $z_k(t)$ in (5) formulating an AM–FM model.

ESTIMATING THE IF OF MULTICOMPONENT SIGNALS

BASIC APPROACH TO IF ESTIMATION

Here, the TFD of the signal is calculated using a reduced interference TFD (RI-TFD) and is then transformed into a 2-D binary image [1], [6], [7]. The maximum peaks in the TFD are found using the first and second derivatives with respect to frequency. The peaks that are larger than a threshold are marked by one while all the other points in the

representation are marked by zero. These peaks are potential IFs; they are linked by searching the next peak within a neighboring set [component linking (CPL)] [8]. The linked peaks are defined as a true component if their time duration is longer than a predetermined threshold, which depends on the minimum length that a signal component could be.

THESE THEORETICAL DEVELOPMENTS AND TECHNIQUES HIGHLIGHT THE IMPORTANCE OF CONTINUING TO DEVELOP, ADAPT, AND APPLY NEW HIGH-RESOLUTION T-F METHODS FOR DIAGNOSTIC APPLICATIONS.

COMPONENT EXTRACTION TECHNIQUES

Another approach for estimating the IF of a multicomponent signal is to first extract the signal components from its TFD using methods such as blind source separation (empirical mode decomposition can also be used for extracting signal components, but it is not used in this work due to its mode-mixing problem and sensitivity to noise). Once the signal components are extracted from the signal, their IF laws are estimated using monocomponent IF estimation techniques [17]. As the TFD of a multicomponent signal contains cross-terms that complicate the components separation procedure, one chooses an RI-TFD that attenuates cross-terms while preserving the T-F resolution [1], [7].

APPLICATION TO THE ANALYSIS OF EEG AND HRV SIGNALS

The above multicomponent IF estimation techniques are meaningful for EEG and HRV signals. HRV signals, for example, the statistics of the IF laws of HRV signals, can be used to study the automatic nervous regulation of the cardiovascular function [13]. For a newborn's EEG signals, the statistics of the IF laws have shown good performance in detecting newborn EEG abnormalities [8]. For an illustration, Figure 4 shows the estimated IF laws of the newborn EEG and HRV signals shown in Figure 1, using the CPL method.

All the above would require the definition and design of high-resolution QTFDs specifically adapted to particular nonstationary multicomponent signals, especially when the components are very close to each other; this is addressed next.

FORMULATING HIGH-RESOLUTION QTFDs

The WVD is considered an efficient tool for analyzing monocomponent LFM signals, because of its high T-F resolution for such signals [1]. However, due to its bilinear nature, it introduces cross-terms when the signal is multicomponent and/or nonlinear FM. The presence of such cross-terms in QTFDs is a fundamental limitation that prevents more widespread use of WVD-based multicomponent T-F signal analysis in real-life applications.

Attempts to design TFDs that reduce cross-terms while preserving high T-F resolution led to the introduction of RI-TFDs, such as the Gaussian (GD), B (BD), modified-B distributions (MBDs), extended MBD (EMBD), and compact-support kernel TFDs [1], [6], [7]. Among these RI-TFDs, both MBD and EMBD have shown superior performance in analyzing real-life signals such as EEG and HRV signals [7], [18]. These have Doppler-lag kernels of the form $g(\nu,\tau) = G_1(\nu)g_2(\tau)$. These separable kernel TFDs result directly from the estimation of the PSD of a nonstationary signal when no assumption of stationarity is made [1]. A methodology for designing such RI-TFDs is therefore of immediate importance and practical interest. This article approaches this issue by initially focusing on separable and directional compact support kernels.

METHODOLOGY FOR DESIGNING RI-TFDs WITH SEPARABLE KERNELS

The aim is to find $g(\nu,\tau) = G_1(\nu)g_2(\tau)$ such that the TFD in (3) provides a good energy concentration for all components and a good suppression of cross-terms. We denote $g_1(t) = \mathcal{F}^{-1}_{\nu\to t}\{G_1(\nu)\}$ and $G_2(f) = \mathcal{F}_{\tau\to f}\{g_2(\tau)\}$. As the TFD with Doppler-lag kernel

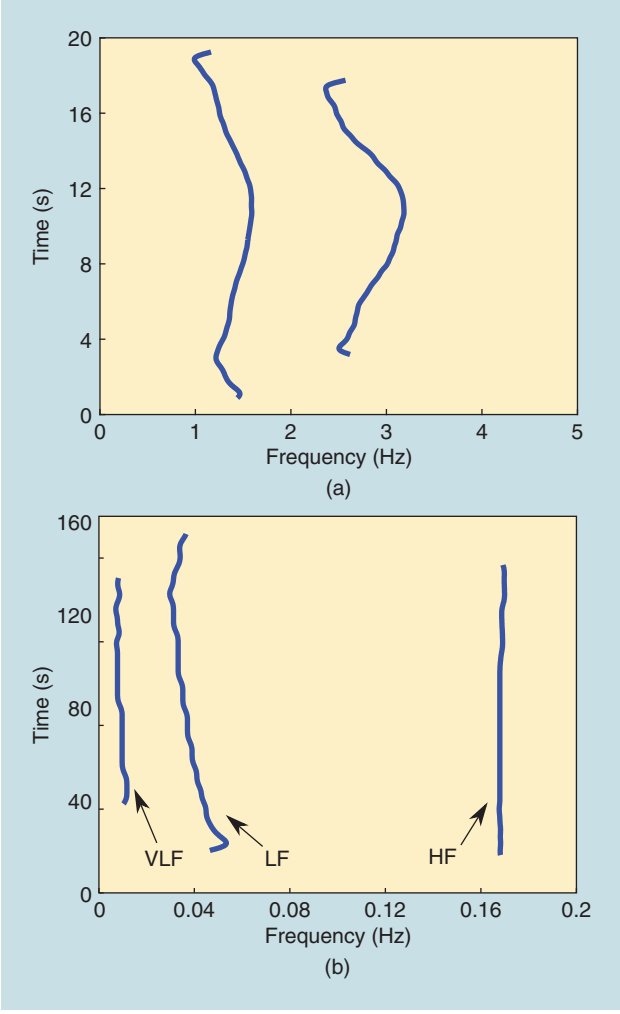

[FIG4] Estimated IF laws of an epoch of (a) newborn EEG and (b) HRV signals shown in Figure 1(a) and (c).

$g(\nu,\tau)$ is real if $g(\nu,\tau) = g^*(-\nu,-\tau)$ [1], if we choose $g_1(t)$ and $g_2(\tau)$ real with $g_2(\tau)$ an even function of τ, then the resulting TFD will be real. The property of total energy is satisfied by choosing $g_1(t)$ and $g_2(\tau)$ such that $g(0,0) = 1$ [1], e.g., $G_1(0) = g_2(0) = 1$, resulting in $\int\int \rho_z(t,f)\mathrm{d}t\mathrm{d}f = E_z$, where E_z is the energy of $z(t)$.

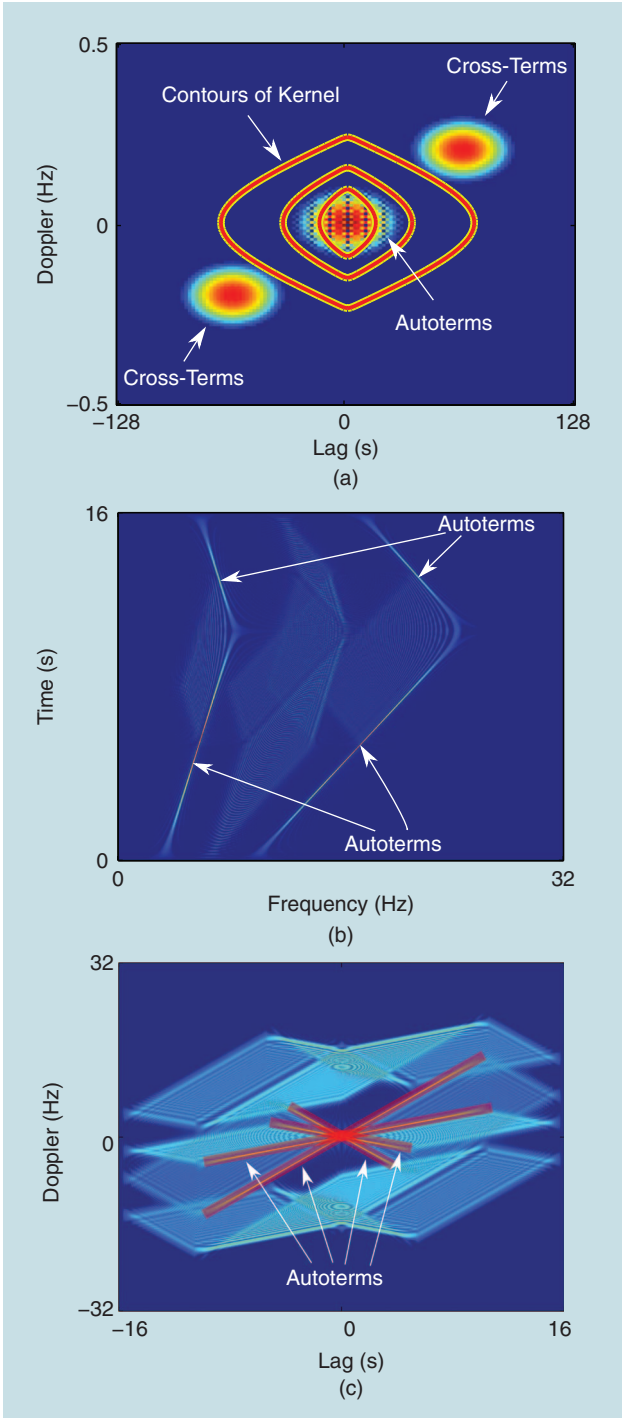

[FIG5] (a) Representations of (6) with $K = 2$, $a(t) = \mathrm{e}^{-t^2/100}$, and $t_1 = 32$ s, $t_2 = 96$ s, $f_1 = 0.1$ Hz, $f_2 = 0.3$ Hz. As shown, using the EMBD kernel given in (9) with $\alpha = 0.02$ and $\beta = 0.6$, cross-terms can be filtered out without attenuating auto-terms; (b) WVD of a piecewise LFM signal consisting of four components; and (c) SAF of the signal shown in (b). The autoterms in the AF are highlighted with a red rectangle.

To understand how TFDs perform for multicomponent signals, we consider a simple case of the model in (5) where the signal components are time-delayed frequency-shifted versions of a low-pass envelope $a(t)$, i.e.,

$$z_K(t) = \sum_{k=1}^{K} a(t - t_k)e^{j2\pi f_k t}, \tag{6}$$

where t_k and $f_k, i = 1,2,...,K$ are constants. Note that the SAF $A_a(\nu,\tau)$ is located around the origin in the Doppler-lag domain [1]. Then $A_{z_K}(\nu,\tau)$ can be expressed as shown in (7)

$$\begin{aligned} A_{z_K}(\nu,\tau) = A_a(\nu,\tau)\sum_{k=1}^{K} e^{j2\pi(f_k\tau - t_k\nu)} \\ + \sum_{k=1}^{K}\sum_{\substack{l=1 \\ l\neq k}}^{K} A_a(\nu-(f_k-f_l),\tau-(t_k-t_l)) \\ e^{j2\pi\left(\frac{f_k+f_l}{2}\tau - \frac{t_k+t_l}{2}\nu + (f_k-f_l)\frac{t_k+t_l}{2}\right)}. \end{aligned} \tag{7}$$

Equation (7) shows that the first term representing the autoterms maps to the origin, while the second term representing the cross-terms in general maps away from the origin, relatively. For an illustration, Figure 5(a) shows a two-component signal in the ambiguity domain. For cases similar to Figure 5(a), (7) also shows that the closest cross-term to the origin is located at $(|\min(f_k - f_l)|, |\min(t_k - t_l)|); l \neq k$ in the Doppler-lag domain. These facts suggest that for effective attenuation of cross-terms 1) both $G_1(\nu)$ and $g_2(\tau)$ need to be "low-pass" and 2) their amplitudes need to be significantly small (ideally zero) for $\nu^2 \geq \nu_0^2$ and $\tau^2 \geq \tau_0^2$, where $\nu_0 = |\min(f_k - f_l)|$, $l \neq k$ and $\tau_0 = |\min(t_k - t_l)|$, $l \neq k$.

Several window functions can be used to define a Doppler-lag kernel satisfying the above requirements. Among them are hyperbolic: $h_\alpha(t) = \cosh^{-2\alpha}(t)$, Gaussian: $h_\alpha(t) = \mathrm{e}^{-(\pi\alpha t)^2}$, sinc: $h_\alpha(t) = \mathrm{sinc}^2(\alpha t)$, and Cauchy: $h_\alpha(t) = \alpha^2(\alpha^2 + t^2)^{-1}$ windows. The general form of a separable-kernel TFD can then be given by (3) with

$$g(\nu,\tau) = g_2(\tau)G_1(\nu) = h_\alpha(\tau)\frac{\int_{-\infty}^{\infty} h_\beta(t)\mathrm{e}^{\mathrm{j}2\pi\nu t}\mathrm{d}t}{\int_{-\infty}^{\infty} h_\beta(t)\mathrm{d}t}. \tag{8}$$

Note that the resulting TFD is real and satisfies the total energy property (as $G_1(0) = g_2(0) = 1$).

For cases where the energy concentration occurs along the Doppler axis in the ambiguity domain (e.g., the signal given in (6) with $t_k \simeq 0$), the above formulation suggests that the cross-terms can be attenuated using a lag-independent kernel, i.e., $g(\nu,\tau) = G_1(\nu)$, e.g., with $G_1(\nu) = (\int \cosh^{-2\beta}(t)\,\mathrm{e}^{\mathrm{j}2\pi\nu t}\mathrm{d}t)/(\int \cosh^{-2\beta}(t)\mathrm{d}t)$, the MBD is obtained [1].

The above formulations suggest that lag-independent methods like MBD are optimal when the angle between the IF laws and t-axis is zero. Figure 1(c) is such an example where the T-F energy

concentration follows three IF laws that can be described by piecewise linear laws [see Figure 4(b)]. A key question is therefore, how to extend TFDs so that they are optimal for T-F energy concentration directions away from the vertical axis such as the synthetic EEG signal shown in Figure 5(b) where four components join to model a piecewise linear IF law. Figure 5(c) shows the components and the complicated structure of the cross-terms in the SAF. A solution to deal with such signals is described in [7] in which a modification of BD and MBD—EMBD—is proposed to improve performance. The Doppler-lag kernel of this TFD is defined as

$$g(\nu,\tau)=\frac{\int_{-\infty}^{\infty}\cosh^{-2\beta}(t)e^{j2\pi\nu t}dt}{\int_{-\infty}^{\infty}\cosh^{-2\beta}(t)dt}\cosh^{-2\alpha}(\tau). \quad (9)$$

This TFD uses the same window functions for both $g_1(t)$ and $g_2(\tau)$ with two control parameters for better control of the tradeoff between cross-terms attenuation and T-F resolution [7].

EXTENSION TO RI-TFDs WITH COMPACT-SUPPORT KERNELS

As mentioned earlier, in the representation of the signal $z_N(t)$ in (6), the closest cross-term appears at a certain point (ν_0,τ_0) in the Doppler-lag domain. Thus, for effective removal of cross-terms, one should choose the control parameters of the kernel such that

$$G_1(\nu)=0;\ \text{for}\ \nu^2\geq\nu_0^2\ \text{and}\ g_2(\tau)=0;\ \text{for}\ \tau^2\geq\tau_0^2. \quad (10)$$

Therefore, for kernels $G_1(\nu)g_2(\tau)$, when given signal components are very close in t-domain and/or f-domain, to achieve effective attenuation of cross-terms, one should choose the control parameters of the kernel very small (i.e., close to zero). This in turn results in autoterms attenuation and loss of resolution. The control parameters need therefore to mediate the tradeoff between cross-term elimination and T-F resolution preservation. According to (10), one way to solve the above problem and obtain maximum cross-term attenuation and T-F resolution simultaneously is to define the TFD kernel such that it is in fact zero for $\nu^2\geq\nu_0^2$ and $\tau^2\geq\tau_0^2$, resulting in compact-support kernels such as those in [6].

EXTENSION TO RI-TFDs WITH NONSEPARABLE KERNELS

In some conditions, the requirement of TFD optimality leads to a kernel that cannot be separable. Such situations occur, e.g., when the T-F energy concentration defines a direction in the T-F plane that is away from one of the axes. An example of such a nonseparable kernel is presented in [7]. A natural improvement is to use TFDs with directional compact support kernels to deal with such situations. This can be done by designing directional filters that take into account the privileged directions in the ambiguity domain where the energy of the signal autoterms concentrate, as illustrated by Figure 5(c). To do this may require revisiting and extending methods such as the adaptive method in [19] or [20]. This is particularly important in newborn EEG seizure detection applications, as previous studies found that such signals can be modeled as a multicomponent piecewise LFM signal whose SAF will have similar characteristics to Figure 5(c). For all such scenarios, there is always a tradeoff between cross-terms attenuation and T-F resolution. Note that the above heuristic and conceptual approach also relates to the tradeoff between the stationarity assumption (which is global) and the local ergodicity assumption, therefore affecting the design of $g_1(t)$ and $g_2(\tau)$ [1], [21].

THREE PROBLEMS MAY ARISE WITH DISCRETE TFDs: ALIASING, LOST MATHEMATICAL PROPERTIES, AND EXCESSIVE COMPUTATIONAL LOAD OR MEMORY REQUIREMENTS.

DISCRETE FORMULATION OF TFDs

The TFD in (3) is defined in the continuous domain for infinite-length signals. For digital implementation, the TFD is transformed from the continuous to the discrete domain and the infinite signals are made finite. Three problems may arise with discrete TFDs: aliasing, lost mathematical properties, and excessive computational load or memory requirements.

By careful implementation of the analytic signal and TFD [1, Sec. 6.1], [22], the aliasing can be reduced. The analytic signal is ideally zero for one-half of its time-duration and one-half of its spectrum [1] to avoid overlap (aliasing) in the discrete T-F domain. A natural approach to defining the discrete analytic signal, with a reduction in aliasing in the T-F domain of approximately 50%, for real-valued signal $s[n]$ of length N, is to 1) zero-pad $s[n]$ from length N to length $2N$, then 2) zero negative frequencies for $s[n]$, and finally 3) let $z[n]=s[n]$ for $0\leq n\leq N-1$ and $z[n]=0$ for $N\leq n\leq 2N-1$.

To implement the discrete version of the TFD in (3) requires addressing the problem that the discrete signal does not have samples at lag values of $\tau/2$ [see (2) and (3)]. A discrete definition of a TFD, which satisfies important mathematical properties such as the frequency-marginal property, is defined for signals of length N as [1], [22]

$$\rho[n,k]=\left(W[n,k]\circledast_n\circledast_k\gamma[n,k]\right)\Big|_{k=0,1,\ldots,N-1}$$
$$\text{with}\ W[n,k]=\sum_{m=0}^{2N-1}K[n,m]e^{-j2\pi mk/2N}, \quad (11)$$

where $\circledast$ represents circular convolution, $W[n,k]$ the discrete WVD, and $K[n,m]$ represents a discrete version of $K(t,\tau)=z(t+\tau/2)z^*(t-\tau/2)$. This time-lag function is defined on a nonuniform discrete grid as $K[2n,2m]=z[n+m]z^*[n-m]$ and $K[2n+1,2m+1]=z[n+m+1]z^*[n-m]$ and zero elsewhere; i.e., $K[2n,2m+1]=0$ and $K[2n+1,2m]=0$. This

nonuniform discrete grid includes all signal samples: $K[n,m]$ contains values of $z[c]z^*[d]$, for c and d both even, both odd, or either c even and d odd, or c odd and d even. A consequence of including the product of the even-odd index-terms in the time-lag function is that all sample points of the discrete signal are included and the discrete TFD then satisfies all desired important properties, such as t and f marginals, signal recovery, and Moyal's formula [1, Sec. 6.1], [22].

STUDIES SHOW THAT NEWBORN EEG SEIZURES CAN BE MODELED AS PIECEWISE LFM SIGNALS WITH HARMONICS, WHERE THE NUMBER OF LFM PIECES DEPENDS ON THE DURATION OF THE EEG SEIZURE EPOCH.

ALGORITHMS FOR TFDs

TFDs require significant time and memory to compute and store in digital devices, such as personal computers or field programmable gate arrays (FPGAs), especially for medical physiological signals, when long-duration recordings or multiple sensors can create large data sets. For example, a sick newborn with a birth-related brain injury requires neuroprotective treatment promptly to limit brain injury; there is therefore a need to optimize TFD algorithms in terms of computation speed [1]. The separable-kernel TFD [see (8)] is usually oversampled when the length of $g_2(\tau)$ and $G_1(\nu)$, P and Q, are smaller than the length of the signal (N). Eliminating oversampling significantly reduces computations and memory required to compute the TFD: computational complexity reduces from $O(N^2 \log N)$ to $O(PN \log N)$ and memory reduces from $2N^2$ sample points to QP sample points; for example, 1 s of speech, sampled at 16 kHz, requires 5.4×10^9 bytes of memory to store the oversampled $2N \times N$ discrete TFD (assuming one sample point requires 8 bytes for storage); with $P = 255$ and $Q = 511$, the separable-kernel TFD algorithms can compute and store the $2Q \times P/2$ distribution with only 1×10^6 bytes (a difference of three orders of magnitude, i.e., one million less) [22].

TIME-FREQUENCY DETECTION OF ABNORMALITIES IN NONSTATIONARY SIGNALS

A GENERAL APPROACH TO T-F MATCHED FILTER DESIGN

Using the TFDs previously designed, we reconsider the classical detection problem where a measured signal $x(t)$ of duration T is processed to detect the presence of a known signal representing a particular abnormality. The two possible hypothesis on $x(t)$ are as follows:

$$\begin{aligned} &H_0 : x(t) = n(t), && \text{abnormality signal absent,} \\ &H_1 : x(t) = s(t;\Theta) + n(t), && \text{abnormality signal present,} \end{aligned} \tag{12}$$

where $n(t)$ represents additive noise and $s(t;\Theta)$ is a known deterministic signal representing an abnormality dependent on unknown parameters Θ. The optimum decision strategy for the detection problem in (12) involves finding a test statistic such as

$$\eta = \max_{\Theta} \left\{ \int_{(T)} x(t) s^*(t;\Theta) \mathrm{d}t \right\}$$

and comparing it with a predefined threshold to determine correct hypothesis [23].

Assuming there is no unknown parameters and noise $n(t)$ is a zero mean white Gaussian process, based on the inner-product invariance property of the WVD [1, p. 62], the optimum test statistic in terms of analytic associates $z_x(t)$ and $z_s(t)$ is expressed as

$$\eta_{\mathrm{QMF}} = \left| \int_{(T)} z_x(t) z_s^*(t)\, \mathrm{d}t \right|^2 = \iint_{(T)} W_{z_x}(t,f) W_{z_s}(t,f) \mathrm{d}t\, \mathrm{d}f, \tag{13}$$

which is known as the quadrature matched filter (QMF). When the signal-to-detect $s(t)$ is deterministic and known, i.e., $s(t) = d(t)$, the filter with test statistic given by (13) is optimum.

T-F KERNEL SELECTION FOR PERFORMANCE ENHANCEMENT

A limitation to the above is that in most real-life examples, the signal-to-detect is neither deterministic nor known completely. One such case is when $s(t)$ is a time-delayed frequency-shifted version of $d(t)$, i.e., $s(t) = d(t-t')e^{\mathrm{j}2\pi f' t}$, where $d(t)$ is known and deterministic and t' and f' are random variables with joint probability density function (p.d.f.) $\gamma(t,f)$. For this scenario, the optimum solution is the TFMF with the following test statistic:

$$\eta_{\mathrm{TF}}^{(\mathrm{WV})} = \iint_{(T)} W_{z_x}(t,f) \rho_{z_s}(t,f) \mathrm{d}t\, \mathrm{d}f \tag{14}$$

with $\gamma(t',f')$ as the T-F kernel of the TFD [23]. The TFMF with the test statistic given in (14) is a generalized form of QMF. The choice of different kernels $g(\nu,\tau)$ in (14) results in different test statistics; e.g., the Doppler-lag kernel $|g(\nu,\tau)|^2 e^{-\mathrm{j}2\pi t_0 \nu} e^{\mathrm{j}2\pi f_0 \tau}$ results in

$$\eta_{\mathrm{TF}}^{(\mathrm{WV})} = \iint_{(T)} \rho_x(t,f) \rho_s(t-t_0, f-f_0) \mathrm{d}t\, \mathrm{d}f,$$

which has been used in [1] and [9] for newborn EEG seizure detection. By replacing $W_{z_x}(t,f)$ in (14) with the XWVD of the signals $x(t)$ and $s(t)$, i.e., $W_{z_x z_s}(t,f)$, the test statistic of the general formulation of TFMF based on the XWVD is derived which has shown better noise performance than the one based on (14) [23].

Studies show that, if signal $s(t)$ is not known and can only be inferred from noisy measurements or, if $s(t)$ is randomly perturbed in some way, TFMFs can outperform the filter with test statistic given in (13) [9]. The effect of different T-F kernels on the performance of TFMF based on XWVD for newborn seizure detection is studied quantitatively in the next section.

ILLUSTRATION ON NEWBORN SEIZURE DETECTION

Studies show that newborn EEG seizures can be modeled as piecewise LFM signals with harmonics, where the number of LFM pieces depends on the duration of the EEG seizure epoch [e.g., Figure 1(a)] [9]. Background patterns, on the other hand, usually exhibit irregular activities with no clearly consistent behavior [1]. So, newborn EEG seizure detection can be done by detecting the presence of piecewise LFM signals with unknown parameters (e.g., time-delay and/or frequency-shift) in newborn EEG signals as per (12) [1].

FEATURES USING THE INFORMATION IN THE T-F DOMAIN CAN IDENTIFY SIGNALS' NONSTATIONARY CHARACTERISTICS BASED EITHER ON SIGNAL CHARACTERISTICS SUCH AS IF OR ON IMAGE DESCRIPTORS.

EEG DATA ACQUISITION AND PREPROCESSING

A newborn multichannel EEG database, i.e., EEG-DB, with $C = 20$ channels of continuous EEG recordings of five neonates using bipolar montage according to the 10–20 standard is used. The signals are recorded using a Medelec Profile system at a 256-Hz sampling rate and marked for seizures by a pediatric neurologist from the Royal Children's Hospital in Brisbane, Australia. The EEG signals are first filtered in [0.5 16] Hz, as newborn EEG seizures have spectral activities mostly below 12 Hz [8]. The filtered signals are then downsampled at 32 Hz to minimize computations. Finally, the signals are segmented using a rectangular window of length 8 s, resulting in EEG segments with $N = 256$ samples.

TFMF APPROACH FOR SEIZURE DETECTION IN NEWBORN EEG

The above T-F matched filtering approach is applied here to detect seizures in newborn multichannel EEGs. An arbitrary segment of multichannel EEG signal is composed of C channels as $\mathbf{eeg}(t) = (\mathrm{eeg}_1(t)\ \mathrm{eeg}_2(t)\ \cdots\ \mathrm{eeg}_C(t));\ 0 \le t \le T$ where T is the segment length. The template set is assumed to be composed of J seizurelike events and is denoted as $\mathbf{r}(t) = \{r_j(t)\}_{j=1}^{J}$.

Template Set

The idea is to define templates to best represent the range of seizure types, as too many templates increase computations and probability of error, while too few increase false negatives. The template set contains seizurelike events, which can be modeled by LFM signals if EEG signals are segmented into relatively short epochs (e.g., 8 s long) [9]. For example, a template set can be composed of $J = 3$ LFM signals

$$r_j(t) = \mathrm{e}^{-\mathrm{j}\,\pi\left(2f_0 t + \alpha_j (t - \frac{T}{2})^2\right)};\ 0 \le t \le T;\ j = 1,2,3, \qquad (15)$$

where $\alpha_j \in \{-0.05, 0, 0.05\}$. As observed in (15), $r_2(t)$ has a constant IF law and the others have linearly increasing and decreasing IF laws. When analyzing the kth channel of $\mathbf{eeg}(t)$, i.e., $\mathrm{eeg}_k(t)$, the frequency f_0 is found as the frequency at which the time slice of $\mathrm{eeg}_k(t)$ at $t = T/2$ attains its peak. Note that f_0 may be different for signals acquired from different channels as they may have different T-F signatures. With this approach, f_0 is found based on the fundamental component in $\mathrm{eeg}_k(t)$. This is because the energy of the harmonics in $\mathrm{eeg}_k(t)$ is relatively small compared to that of the fundamental component [9].

Methodology

For each EEG segment $\mathrm{eeg}_k(t)$ with TFD $\rho_{\mathrm{eeg}_k}(t, f)$, three templates are formed using (15). The test statistic of the TFMF is based on the XWVD and is given by

$$\mu^{(k)} = \max_{r_j} \left\{ \iint_{(T)} \left| W_{\mathrm{eeg}_k, r_j}(t, f) \right| \rho_{r_j}(t, f)\, \mathrm{d}t\, \mathrm{d}f \right\}. \qquad (16)$$

As $W_{\mathrm{eeg}_k, r_j}(t, f)$ is not necessarily real, its modulus is used. The test statistic is normalized to [0, 1], and compared with a threshold to find the binary decision value for the kth channel; if a seizure is detected in one of the channels, then $\mathbf{eeg}(t)$ is labeled as a seizure.

Performance Evaluation

Consider the same multichannel EEG database EEG-DB; the performance criterion for each T-F kernel is the area under the receiver operation characteristic graph (i.e., AUC). The AUCs for the spectogram (SPEC) (with Bartlet window length of 127 samples) and MBD with $(\beta = 0.01)$ are 0.94 and 0.95, respectively. The t-domain matched filter has an AUC score of 0.87, indicating that TFMF-based detectors based on high-resolution TFDs offer high performance due to the T-F kernel dealing with the unknown parameters of the signals-to-detect.

T-F-BASED FEATURES FOR CLASSIFYING MULTICOMPONENT NONSTATIONARY SIGNALS

Features using the information in the T-F domain can identify signals' nonstationary characteristics (as in Figure 1) based either on signal characteristics such as IF or on image descriptors.

T-F SIGNAL-RELATED FEATURES

Signal-related features are directly related to signal parameters. Consider an N-point signal, with discrete TFD $\rho[n, k]$ represented by an $N \times M$ matrix $\boldsymbol{\rho}$, where M is the number of FFT points used in calculating $\rho[n, k]$; the following features can be defined:

1) The energy concentration measure shows how the signal energy is distributed over the T-F plane [24]. It is given by

$$F_{R_1} = \left(\sum_{n=1}^{N} \sum_{k=1}^{M} |\rho[n, k]|^{\frac{1}{2}} \right)^2. \qquad (17)$$

2) The T-F Renyi entropy is given by

$$F_{R_2} = 1/1 - \alpha \log\left(\textstyle\sum_{n=1}^{N} \sum_{k=1}^{M} \rho[n, k] / \sum_n \sum_k \rho[n, k] \right).$$

3) T-F complexity measure uses both singular value decomposition (SVD), and Shannon entropy and is based on the

singular values of the matrix $\boldsymbol{\rho}$, i.e., $S_i, i = 1,2,\cdots,N$. It represents the magnitude and the number of the nonzero singular values of the TFD of nonstationary signals and is given by $F_{R_3} = -\sum_{i=1}^{N} \overline{S}i \log_2(\overline{S}i)$, where $\overline{S}i, i = 1,2,\cdots,N$ are the normalized singular values of the matrix $\boldsymbol{\rho}$.

4) SVD-based features are also extracted from the singular values of the matrix $\boldsymbol{\rho}$. The maximum and variance of the singular values, denoted as F_{R_4} and F_{R_5} respectively, can be chosen as characteristic features of the singular values of $\boldsymbol{\rho}$.

DISTINGUISHING BETWEEN ICTAL AND NONICTAL PLEDs IS CRUCIAL TO AID DIAGNOSIS AND TREATMENT DECISIONS; THIS CAN BE DONE BY USING IF MEASUREMENTS.

5) IF-based features are based on the statistics of the IF, such as its mean, i.e., F_{R_6}, its deviation, i.e., $F_{R_7} = \max(f_i[n]) - \min(f_i[n])$, variance, skewness, and kurtosis.

6) Time-varying spectral flatness is an extension of the concept of spectral flatness to nonstationary signals and can be defined as

$$\text{TVSF} = \left(\prod_{k=1}^{M} \rho[n,k]\right)^{M^{-1}} / M^{-1} \sum_{k=1}^{M} \rho[n,k].$$

For example, the mean and deviation of TVSF, i.e., F_{R_8} and F_{R_9}, can be used as characteristic features.

7) The number of signal components is calculated as $F_{R_{10}} = 2^{F_{R_{2\text{signal}}} - F_{R_{2\text{reference}}}}$ [8].

Other signal related features include those presented in [11], and [25]–[27].

T-F IMAGE-RELATED FEATURES

Image-related features are image descriptors extracted from T-F images, i.e., the TFDs considered as images. Such T-F image processing techniques detect regions from the TFD image where all important information, to be detected or identified, appear (e.g., IF and energy concentration pattern) and then extract the features which describe visually this information. One such technique is watershed segmentation, which detects homogeneous regions in the T-F image and then computes their statistical and geometrical features [8].

Morphometric features can be extracted from the moments of the binary segmented TFD image $\rho^{(\text{seg})}[n,k]$ with moment of order (p,q) for $\rho^{(\text{seg})}[n,k]$ expressed as $m_{pq} = \sum_n \sum_k n^p k^q \rho^{(\text{seg})}[n,k]$, where $p,q = 0,1,2,\ldots$. Using m_{pq}, we can define morphometric features such as area: $F_{I_1} = m_{00}$, compactness: $F_{I_2} = P^2/F_{I_1}$ where $P = (m_{30}+m_{12})^2 + (m_{03}+m_{21})^2$, coordinates of the centroid for the segmented region: $F_{I_3} = m_{10}/m_{00}$ and $F_{I_4} = m_{01}/m_{00}$, rectangularity: $F_{I_5} = (m_{20}-m_{02})^2 + 4m_{11}^2$, and aspect ratio: $F_{I_6} = m_{20} - m_{02}$ [8].

ILLUSTRATION ON NEWBORN SEIZURE DETECTION

METHODOLOGY

To evaluate the performance of a T-F feature, e.g., F_{R_1}, consider a segment of multichannel EEG signal $\text{eeg}(t)$ and a given T-F kernel, with TFDs $(\rho_{\text{eeg}_1}[n,k],\ldots,\rho_{\text{eeg}_C}[n,k])$. From each TFD we evaluate the feature using (17) and find $\mathbf{F}_{R_1} = (F_{R_1}^{(1)},\ldots,F_{R_1}^{(C)})$, where $F_{R_1}^{(k)}$ is the feature value extracted from the EEG signal recorded from the kth channel. Finally, the receiver operating characteristic (ROC) is found for $|\mathbf{F}_{R_1}|$ and the resulting AUC, i.e., $\text{AUC}_{\mathbf{F}_{R_1}}$ is calculated.

PERFORMANCE EVALUATION

Using the database EEG-DB, the performance of T-F features is evaluated for each TFD by computing the average AUCs for signal- and image-related features, i.e., $\overline{\text{AUC}_\text{R}} = 1/10\sum_{i=1}^{10} \text{AUC}_{\mathbf{F}_{Ri}}$ and $\overline{\text{AUC}_\text{I}} = 1/6\sum_{i=1}^{6} \text{AUC}_{\mathbf{F}_{Ii}}$. For SPEC with a Bartlet window of length 127 samples, MBD with $\beta = 0.01$, EMBD with $\alpha = 0.9$ and $\beta = 0.01$ and WVD, $\overline{\text{AUC}_\text{R}}$ (respectively $\overline{\text{AUC}_\text{I}}$) are 0.84 (0.70), 0.80 (0.59), 0.66 (0.62), and 0.66 (0.57). For EMBD, the best performing signal- and image-related features are F_{R_9} and F_{I_4}, respectively, with maximum 0.75 and 0.83 AUC scores. The results indicate that the T-F features extracted from high-resolution TFDs outperform those extracted from WVD. Also, for the problem of newborn EEG seizure detection, comparing the AUC results of T-F-based features with those of the TFMFs, we observe that T-F features perform as good as TFMFs with much less computational load.

EXAMPLES OF T-F APPLICATIONS FOR AUTOMATING MEDICAL ABNORMALITY DIAGNOSIS

T-F CLASSIFICATION OF ECG/HRV SIGNALS

Perinatal hypoxia is a condition resulting from the deficiency of oxygen supply to a tissue below physiological levels despite adequate perfusion of the tissue by blood. It is a major cause of cerebral injury, accounting for a large amount of morbidity and mortality in newborns [13]. Early detection of hypoxia is of great clinical importance to reduce the risk of adverse outcomes following an injury and to help clinicians plan and conduct appropriate therapeutic strategies promptly to minimize brain injury. This can be done by automatic hypoxia detection method using T-F features extracted from HRV signals.

EXPERIMENT AND DATA RECORDING

This study used 21 newborn piglets under hypoxic condition to simulate perinatal hypoxia in human babies because piglets have similar ontogenesis of nervous and cardiovascular systems to human babies [28]. Such an experiment with controlled hypoxia enables an accurate annotation of the data, a necessary requirement for evaluating the effectiveness of the analysis methods. Five minute epochs of electrocardiograms (ECGs) before and at the beginning of the hypoxic insult are converted to HRV signals [28].

T-F FEATURE EXTRACTION

Figures 1(c) and 4(b) show that HRV signals can be modeled by three recognizable components. The HF component is

related to respiration, LF component is related to sympathetic and vagal nervous regulation, and VLF component is related to thermoregulation [12], [13]. The components are extracted from the MBD and EMBD of each HRV epoch using the CPL algorithm. Note that WVD is not used due to the presence of cross-terms in the WVD of HRV signals. For each component, the IF and the value of the TFD at its IF are found using: $f_i(t) = \arg\left\{\max_f(\rho_z(t,f))\right\}$ and $p_i(t) = \rho_z(t, f_i(t))$, respectively, where $p_i(t)$ provides an estimate of the IA of the signal component [1, p. 442]. The mean and standard deviation of $f_i(t)$ and $p_i(t)$ for each signal component are calculated, resulting in four T-F features per component. Since the respiration rate remained constant, due to the subjects being ventilated during the experiment, the IF of the HF component was constant and thus its mean and standard deviation are not used. We therefore use ten T-F features for classifying the HRV signals.

THE RULE-BASED METHOD ASSESSES ENERGY, TIME-DURATION, AND MEAN FREQUENCIES OF THE IF TO ENSURE THAT THE ESTIMATED IF IS THE ACTUAL IF OF THE PLEDs AND NOT SOME OTHER EEG BACKGROUND ACTIVITY.

PERFORMANCE EVALUATION

A support vector machine with Gaussian radial basis kernel [8] classifies the HRV signals of newborn piglets under hypoxic condition using the selected features. The total accuracy for classifiers based on SPEC (with Hanning window of 75 samples), MBD (with $\beta = 0.03$), and EMBD (with $\alpha = 0.6$ and $\beta = 0.02$) are 91.2%, 94.9%, and 91.3%, respectively. These high AUC scores indicate that IF- and IA-based features extracted from high-resolution TFDs of HRV signals can be used for automatic detection of perinatal hypoxia.

T-F APPROACH AS A DIAGNOSIS AID FOR BRAIN INJURY IN ADULT EEG

PLEDs are EEG waveforms associated with brain injury. For some patients, PLEDs are associated with ictal activity (seizures). Distinguishing between ictal and nonictal PLEDs is crucial to aid diagnosis and treatment decisions [29]; this can be done by using IF measurements. For PLED signals, the CPL algorithm shows low IF estimation accuracy, probably due to relatively large levels of background activity within the PLED signals. A three-step T-F approach enhances this IF estimation [29] using 1) a simple spike-enhancement method with a nonlinear energy operator, 2) following transformation to the T-F domain, a homomorphic filter described below removes the spectral modulation in the T-F domain [29], and then 3) using a CPL algorithm estimated tracks, a rule-based method selects two tracks with no time overlap and combines them to form one IF. The rule-based method assesses energy, time-duration, and mean frequencies of the IF to ensure that the estimated IF is the actual IF of the PLEDs and not some other EEG background activity.

The homomorphic filter works as follows: first, transform the high-resolution separable-kernel TFD $\rho(t,f)$ to a time-lag domain, $R(t,\tau) = \mathcal{F}^{-1}_{t\to\tau}\{\log \rho(t,f)\}$. Then, apply a high-pass filter $l(\tau)$ in the time-lag domain $R(t,\tau)$ to remove the spectral modulation, and then invert back to the T-F domain: $\bar{\rho}(t,f) = \exp\{\mathcal{F}_{\tau\to f}\{R(t,\tau)l(\tau)\}\}$. Figure 2 shows an example where the enhanced TFD $\bar{\rho}(t,f)$ provides a more accurate estimate of the IF for the PLED signal. The separable-kernel for $\rho(t,f)$ has a Hamming window for lag function $g_2(\tau)$ and a Hanning window for Doppler function $G_1(\nu)$ [1, p. 128]. This kernel produces a smooth TFD with few ripples around zero, which is important as the method assumes the TFD is nonnegative [29].

The method was tested with EEG data containing PLEDs marked by two expert clinical neurophysiologists. Using 33 PLED epochs taken from eight patients, a time-varying period sequence was constructed and then inverted to represent the true IF of the PLEDs. The IF estimation method was tested against this true IF and showed a lower mean-squared error for 79% of epochs compared to the mean-squared error for the IF estimation using only the CPL algorithm. On a database of 13 patients with PLEDs symptoms, two statistical features of the IFs (kurtosis and skewness) showed a statistical significant difference between the ictal and nonictal PLED groups ($p < 0.005$). In addition, evaluating the synchrony of PLEDs across EEG channels, by assessing the similarity of IF in each channel, also showed a statistical difference ($p < 0.05$). Neither IF mean nor median showed a difference between the two groups, thus emphasizing the need for a T-F analysis approach based on high-resolution TFDs that yield accurate IF estimates.

T-F ENHANCEMENT OF PATHOLOGICAL OESOPHAGEAL SPEECH SIGNALS

Oesophageal speech is an abnormal mode of speaking used by people without a larynx. They speak by expelling air from the stomach through the oesophagus into the vocal tract. The air vibrates the upper segment of the oesophagus, thus mimicking the normal periodic opening and closing of the glottal fold. Such speech sounds rough, harsh, often with low pitch and volume. Speech enhancement can improve its quality and intelligibility and thus help improve quality of life for oesophageal speakers. Such speech is more nonstationary than normal laryngeal speech: it is noisier and the fundamental frequency varies significantly more than with laryngeal speech [30]. Existing methods to enhance oesophageal speech assume that the signal is short-time stationary, and split the signal into a source signal (a model of the glottal signal) and a filter component (a model of the vocal tract) [30]. An improvement is obtained by using quadratic TFDs to transform speech signal $s(t)$ to the T-F domain $\rho_s(t,f)$; and then proceed as follows:

1) divide this TFD into a source component (approximating the glottal source) and a filter component (approximating the vocal tract), using homomorphic filtering in the T-F domain, as in the previous example of PLEDs; note that $\rho_s(t,f) = \rho_{\text{source}}(t,f)\,\rho_{\text{filter}}(t,f)$

2) estimate IF $f_k(t)$, IA $a_k(t)$ and phase difference $\varphi_k(t)$ from the source TFD; a CPL algorithm estimates the IF and amplitude; then estimate the phase as follows:

- using the IF and amplitude parameters, construct signal $x(t)$ using the real part of the sinusoidal model from (5), where $\phi_k(t) = 2\pi \int_0^t f_k(\tau)\mathrm{d}\tau$
- to estimate the phase difference $\varphi(t)$ between $s(t)$ and $x(t)$, form a cross TFD of speech signal $s(t)$ and signal estimate $x(t)$ and use the same locations of the IF components $f_k(t)$ to estimate the phase difference

3) smooth all instantaneous parameter $f_k(t)$, $a_k(t)$, and phase $\varphi_k(t)$ using a low-pass filter and form another signal $y(t)$ using the same model again in (5) with these filtered instantaneous parameters; here $\phi_k(t) = \varphi_k(t) + 2\pi \int_0^t f_k(\tau)\,d\tau$

4) transform $y(t)$ to the T-F domain $\rho_y(t,f)$; and modulate the TFD of $y(t)$ with $\rho_{\text{filter}}(t,f)$ to form a final TFD $\rho_{\text{enhanced}}(t,f) = \rho_y(t,f)\,\rho_{\text{filter}}(t,f)$ (see enhanced TFD in Figure 3)

5) finally, estimate the t-domain signal from $\rho_{\text{enhanced}}(t,f)$ using the above procedure.

Estimating the phase difference is important for reconstructing speech signals to avoid unnatural sounding phase distortion. The method is tested with 23 recordings of the word "mama" by six Spanish oesophageal speakers. For each word sample, its voiced segment was manually identified and a harmonic-to-noise ratio (HNR) was computed. The original word is compared with the enhanced version, using the above method. For all 23 samples, there is an improvement in HNR, with a significant average improvement of 2.81 dB ($p = 1.4 \times 10^{-5}$).

T-F MEASUREMENT OF ASYNCHRONY IN MULTICHANNEL NEWBORN EEG

The quantification of global phase synchronization within multivariate nonstationary signals has an important application for assessing interactions and connectivity between different parts of the human brain using multichannel EEGs (see [14]–[16] and references therein); T-F-based approaches can be used for studying such functional connectivity using EEG and fMRI [3].

Existing methods based on the IP of signals use the unwrapping method to deal with the problem of unpredicted $\pm 2\pi$ jumps between consecutive phase values. To overcome this, an IF-based generalized phase synchrony measure is defined using the concept of cointegration with the linear relationship between the channels IF laws [16]. Consider a multivariate signal of C channels and assume that each channel has Q IF laws estimated from a high-resolution TFD. For the qth; $q = 1,2,...,Q$ IF law of the signal components, the maximum eigenvalues test can estimate the number of cointegrating relationships within the IF laws; $r^{(q)}$; $0 \le r^{(q)} \le C$. The phase synchrony measure is then defined as the normalized number of the cointegrating relationships $r^{(q)}$ given by $\eta = 1/Q.C \sum_{q=1}^{Q} r^{(q)}$; $\eta = 0$ means no cointegrating relationship within IF laws, and $\eta = 1$ means complete phase cointegration within the multivariate signal. Experimental results using a multichannel newborn EEG show a significant increment of the synchrony measure during the seizure periods, meaning that EEG channels are more synchronized within the seizure periods than the nonseizure intervals; thus providing a useful and simple T-F assessment tool.

EEG CHANNELS ARE MORE SYNCHRONIZED WITHIN THE SEIZURE PERIODS THAN THE NONSEIZURE INTERVALS; THUS PROVIDING A USEFUL AND SIMPLE T-F ASSESSMENT TOOL.

CONCLUSIONS AND PERSPECTIVES

This article describes selected medical applications that illustrate great potential in further extending the use of QTFDs as an aid to diagnosis. This requires that new specific research directions be pursued, by defining data-dependent T-F methods, optimizing the parameters of TFD kernels, and modeling signals in the T-F domain. Current studies aim to translate these methods to a clinical setting.

ACKNOWLEDGMENT

This work was funded by the Qatar National Research Fund, grant number NPRP 09-465-2-174.

AUTHORS

Boualem Boashash (b.boashash@uq.edu.au) has published over 500 technical publications that cover digital signal processing and biomedicine. He was one of the early pioneers of the field of T-F signal processing, and he is currently working on medical applications covering newborn EEG analysis as well as ECG, HRV, and fetal movements for improving health outcomes. He is a research professor at the University of Queensland, Centre for Clinical Research, School of Medicine, Brisbane, Australia. He is also currently with the Electrical Engineering Department at Qatar University, where he works on medical projects funded by the Qatar Foundation. He leads an international team that has been working on several funded projects with the objective to design and develop T-F systems in a clinical setting for fetal movement detection, newborn EEG abnormality detection and classification, newborn EEG quality assessment, and improvement using artifact filtering and signal segmentation. He is a Fellow of the IEEE.

Ghasem Azemi (g.azemi@uq.edu.au) received the Ph.D. degree in signal processing from Queensland University of Technology, Brisbane, Australia, in 2004, where he was then employed as a research fellow in T-F signal processing. He then joined the Department of Electrical Engineering at Razi University, Kermanshah, Iran, as an assistant professor. He is now

with the University of Queensland, Centre for Clinical Research, School of Medicine, Brisbane, Australia, as a research fellow working on automatic classification of abnormalities in newborn EEG.

John M. O'Toole (jotoole@ucc.ie) received the Ph.D. degree (2009) from the University of Queensland, Australia, and the B.E. (1997) and M.Eng.Sc. (2000) degrees from the University College Dublin, Ireland. His Ph.D. thesis received the Dean's Award for Outstanding Research. His postdoctoral research has included topics in signal processing and biomedical applications at the Centre for Clinical Research (2008–2010), University of Queensland, Australia; the University of Deusto (2010–2013), Spain; and the Neonatal Brain Research Group (2013–present), University College Cork, Ireland.

REFERENCES

[1] B. Boashash, Ed., *Time-Frequency Signal Analysis and Processing: A Comprehensive Reference*. Oxford, UK: Elsevier, 2003.

[2] P. C. Petrantonakis and L. J. Hadjileontiadis, "Adaptive emotional information retrieval from EEG signals in the time-frequency domain," *IEEE Trans. Signal Processing*, vol. 60, no. 5, pp. 2604–2616, 2012.

[3] C. F. Lu, S. Teng, C. I. Hung, P. J. Tseng, L. T. Lin, P. L. Lee, and Y. T. Wu, "Reorganization of functional connectivity during the motor task using EEG time-frequency cross mutual information analysis," *Clin. Neurophysiol.*, vol. 122, no. 8, pp. 1569–1579, 2011.

[4] A. T. Tzallas, M. G. Tsipouras, and D. I. Fotiadis, "Epileptic seizure detection in EEGs using time-frequency analysis," *IEEE Trans. Inform. Technol. Biomed.*, vol. 13, no. 5, pp. 703–710, Sept. 2009.

[5] G. Garcia, T. Ebrahimi, and J. Vesin, "Joint time-frequency-space classification of EEG in a brain computer interface application," *EURASIP J. Adv. Signal Processing*, vol. 2003, no. 7, pp. 713–729, 2003.

[6] M. Abed, A. Belouchrani, M. Cheriet, and B. Boashash, "Time-frequency distributions based on compact support kernels: Properties and performance evaluation," *IEEE Trans. Signal Processing*, vol. 60, no. 6, pp. 2814–2827, June 2012.

[7] B. Boashash and T. Ben-Jabeur, "Design of a high-resolution separable-kernel quadratic TFD for improving newborn health outcomes using fetal movement detection," in *Proc. 11th Int. Conf. Information Science, Signal Processing and Their Applications (ISSPA)*, July 2012, pp. 354–359.

[8] B. Boashash, L. Boubchir, and G. Azemi, "A methodology for time-frequency image processing applied to the classification of non-stationary multichannel signals using instantaneous frequency descriptors with application to newborn EEG signals," *EURASIP J. Adv. Signal Processing*, vol. 2012, no. 1, pp. 1–21, 2012.

[9] J. M. O'Toole and B. Boashash, "Time-frequency detection of slowly varying periodic signals with harmonics: Methods and performance evaluation," *EURASIP J. Adv. Signal Processing*, vol. 2011, pp. 5:1–5:16, Jan. 2011.

[10] M. Zivanovic and M. Gonzalez-Izal, "Nonstationary harmonic modeling for ECG removal in surface EMG signals," *IEEE Trans. Biomed. Eng.*, vol. 59, no. 6, pp. 1633–1640, June 2012.

[11] B. Ghoraani and S. Krishnan, "A joint time-frequency and matrix decomposition feature extraction methodology for pathological voice classification," *EURASIP J. Adv. Signal Processing*, vol. 2009, pp. 10:1–10:11, Jan. 2009.

[12] M. Orini, R. Bailon, L. T. Mainardi, P. Laguna, and P. Flandrin, "Characterization of dynamic interactions between cardiovascular signals by time-frequency coherence," *IEEE Trans. Biomed. Eng.*, vol. 59, no. 3, pp. 663–673, Mar. 2012.

[13] L. T. Mainardi, "On the quantification of heart rate variability spectral parameters using time-frequency and time-varying methods," *Philos. Trans. Roy. Soc. London A, Math. Phys. Sci.*, vol. 367, no. 1887, pp. 255–275, 2009.

[14] S. Aviyente and A. Y. Mutlu, "A time-frequency-based approach to phase and phase synchrony estimation," *IEEE Trans. Signal Processing*, vol. 59, no. 7, pp. 3086–3098, July 2011.

[15] R. E. Greenblatt, M. E. Pflieger, and A. E. Ossadtchi, "Connectivity measures applied to human brain electrophysiological data," *J. Neurosci. Methods*, vol. 207, no. 1, pp. 1–16, 2012.

[16] A. Omidvarnia, G. Azemi, P. B. Colditz, and B. Boashash, "A time-frequency based approach for generalized phase synchrony assessment in nonstationary multivariate signals," *Dig. Signal Process.*, vol. 23, no. 3, pp. 780–790, May 2013.

[17] B. Boashash, "Estimating and interpreting the instantaneous frequency of a signal. II. Algorithms and applications," *Proc. IEEE*, vol. 80, no. 4, pp. 540–568, Apr. 1992.

[18] B. Boashash and V. Sucic, "Resolution measure criteria for the objective assessment of the performance of quadratic time-frequency distributions," *IEEE Trans. Signal Processing*, vol. 51, no. 5, pp. 1253–1263, May 2003.

[19] D. L. Jones and R. G. Baraniuk, "An adaptive optimal-kernel time-frequency representation," *IEEE Trans. Signal Processing*, vol. 43, no. 10, pp. 2361–2371, 1995.

[20] B. Ristic and B. Boashash, "Kernel design for time-frequency signal analysis using the Radon transform," *IEEE Trans. Signal Processing*, vol. 41, no. 5, pp. 1996–2008, 1993.

[21] B. Boashash, "Time-frequency signal analysis," in *Advances in Spectrum Estimation*, S. Haykin, Ed. Englewood Cliffs, NJ: Prentice-Hall, 1991, ch. 9, pp. 418–517.

[22] J. M. O' Toole and B. Boashash, "Fast and memory-efficient algorithms for computing quadratic timefrequency distributions," *Appl. Comput. Harmon. Anal.*, vol. 35, no. 2, pp. 350–358, Sept. 2013.

[23] A. M. Sayeed, "Optimal time-frequency detectors," in *Time-Frequency Signal Analysis and Processing: A Comprehensive Reference*, B. Boashash, Ed. Oxford, UK: Elsevier, 2003, ch. 12, Article 12.1, pp. 500–509.

[24] E. Sejdic, I. Djurovic, and J. Jiang, "Time-frequency feature representation using energy concentration: An overview of recent advances," *Elsevier Dig. Signal Process.*, vol. 19, no. 1, pp. 153–183, 2009.

[25] A. F. Quiceno-Manrique, J. I. Godino-Llorente, M. Blanco-Velasco, and G. Castellanos-Dominguez, "Selection of dynamic features based on time-frequency representations for heart murmur detection from phonocardiographic signals," *Ann. Biomed. Eng.*, vol. 38, no. 1, pp. 118–137, Jan. 2010.

[26] C. Guerrero-Mosquera, A. Malanda Trigueros, J. Iriarte Franco, and A. Navia-Vazquez, "New feature extraction approach for epileptic EEG signal detection using time-frequency distributions," *Med. Biol. Eng. Comput.*, vol. 48, no. 4, pp. 321–330, Apr. 2010.

[27] J. D. Martinez-Vargas, J. I. Godino-Llorente, and G. Castellanos-Dominguez, "Time-frequency based feature selection for discrimination of non-stationary biosignals," *EURASIP J. Adv. Signal Processing*, vol. 2012, no. 1, pp. 219, 2012.

[28] S. Dong, B. Boashash, G. Azemi, B. Lingwood, and P. B. Colditz, "Detection of perinatal hypoxia using time-frequency analysis of heart rate variability signals," in *Proc. 38th Int. Conf. Acoustics, Speech, and Signal Processing (ICASSP)*, May 2013, pp. 939–943.

[29] J. M. O'Toole, B. G. Zapirain, I. M. Saiz, A. B. A. Chen, and I. Y. Santamaria, "Estimating the time-varying periodicity of epileptiform discharges in the electroencephalogram," in *Proc. 11th Int. Conf. Information Science, Signal Processing and Their Applications (ISSPA)*, July 2012, pp. 1229–1234.

[30] H. R. Sharifzadeh, I. V. McLoughlin, and F. Ahmadi, "Reconstruction of normal sounding speech for laryngectomy patients through a modified CELP codec," *IEEE Trans. Biomed. Eng.*, vol. 57, no. 10, pp. 2448–2458, Oct. 2010.

[SP]